Bulgarian Chemical Communications, Volume 48, Special Issue D, (pp. 05 – 14) 2016

Preparation and characterization of antibacterial nanofibrous trimethoprim/polyvinylpyrrolidone mats as an oral fast-dissolving drug delivery system

A. Bolouri, A. Mohammad-khah*

Department of Chemistry, Faculty of Science, University of Guilan, Namjoo Street, P.O. Box: 1914, Rasht, Iran

Received May 02, 2016, Revised July 10, 2016

In this work, polymeric nanofibers, loaded with Trimethoprim– an antibiotic model drug- fabricated using electrospinning technique, as a novel method for fast-dissolving drug delivery systems applications. Polyvinylpyrrolidone K90 was used as the fibrous matrix polymer and drug carrier.

Characterization and pharmacological examinations of the specimens were carried out using a variety of techniques such as scanning electron microscope, Fourier transform infrared, differential thermal analysis and *in-vitro* drug release test. Analysis showing the smooth fabricated nanofibers with the average diameters of 220 and 350 nm at W_{PMP}/W_{PVP} of 10 and 20 weight percent, respectively. FTIR and DTA examinations revealed that the drug loses its crystalline state and becomes formulated in a nanofiber contexture amorphously.

Pharmacotechnical tests indicated that fibers are quickly moistened and dissolved in artificial saliva by less than 10 seconds. Accordingly, *in-vitro* drug release of nanofibers is a very prompt process which takes less than 30 s to release, due to the large surface area to mass ratio of nanofibers.

In-vitro bacterial inhibition test was also carried out to determine the relative activity of the released antibiotic. Results demonstrated that the medicated TMP/PVP nanofibers have an effective role in inhibiting the growth of bacteria.

Keywords: Electrospinning; Fast-dissolving Drug Delivery System; Polyvinylpyrrolidone; Nanofibers; Trimethoprim.

INTRODUCTION

There has been huge and increasing demand for patient convenient, fast and more effective forms of drugs during the past few decades. Fast-dissolving drug delivery systems (FDDSs) which may release drugs in the mouth, seems to be a promising and rapidly growing area in the pharmaceutical industry which had introduced in 1970s [1-3], in order to facilitate difficulties in swallowing traditional oral solid-dosed forms of drugs for pediatric and geriatric patients. There are many advantages of utilizing FDDS in pharmacology including; bioavailability, fast absorbability, rapid onset of action [4-6], site-specific effect (for example; sore throat) [7-9], precise dosing in addition to pleasant mouth feeling, ease of handling and transportability [10]. In this system, a palatal ligature, which is thin and easily set on the subject's tongue, forms a delivery system. The tablet where designed in FDDS is supposed to be dissolved in saliva causes its immediate hydration and sticking to the stead of the applications as fast as just a few seconds. It subsequently breaks up and deliquesces to extricate the medicine for mucosal and gastrointestinal absorption [11-13].

In drug delivery systems (DDSs), biocompatible and biodegradable polymers can be loaded with different drugs. However, many filaments forming polymers are not suitable for oral performance and only a few polymer excipients can meet the pharmaceutical requirements for developing oral DDSs. Polyvinylpyrrolidone (PVP) as a non-crystalline vinyl polymer (Fig. 1), is possesses potentially diverse functions and benefits in the medical and drug delivery fields, due to diverse material properties such as stickiness, immense physiological consistency, low toxicity and sufficient solubility in water and most organic solvents [14]. Therefore, PVP can be used as a mat for possible oral delivery applications.

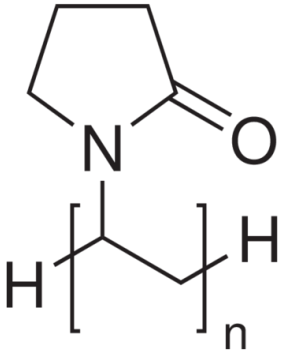

Fig 1. Chemical structure of polyvinylpyrrolidone.

Furthermore, applying nanotechnology and nanostructured materials can help the functionality of the membrane. Nanofibers, as potential

To whom all correspondence should be sent:
E-mail: mohammadkhah@guilan.ac.ir

candidates for implementation in drug delivery membranes, are showing marvelous characteristics and attracting a lot of attentions due to high surface area to mass ratio, the tiny size of inter-fibrous pores with high porosity and possibilities for surface functionalization [15, 16].

Active pharmaceutical ingredient (API)-loaded nanofibers, reported by Kenawy and colleagues in 2002 [17], which mostly used for treatment of external surfaces of the human body, for instance, auxiliary therapy, transdermal DDSs and wound dressing [18-20], can be applied for oral FDDSs [12, 21, 22], although there are very limited reports in this area. Additionally, this technique can be used in a different variety of drugs from analgesics to neuroleptics and anti-psychotics due to its advantages and commonly used in drug delivery market [23, 24].

In this work Electrospinning (ES) technique has been used for fabrication of nanofibers thanks to its simpleness, cost effectiveness as well as ability to produce nanostructures continuously [25, 26]. This technique is adaptable to the wide variety of fields, especially to pharmaceutical [27-29] and biomedical [30-32] applications. Moreover, it is applicable to the most of the soluble or melted biodegradable polymers [33-35]. These specifications make the ES process probably the most suitable option for concocting such formulations.

In this technique, the high voltage direct current (DC) source is applying to induce the charge on the surface of a polymer solution, which is flowing out from a nozzle, and leading to the formation of a jet. Because of the bending instability, the jet is subsequently stretched and forms continuous and ultrathin fibers (Fig. 2) [36].

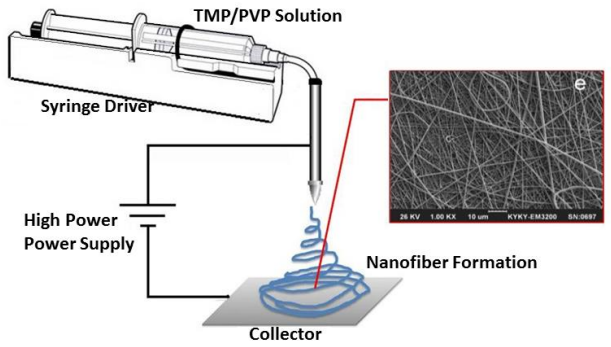

Fig 2. Schematic illustration of electrospinning setup.

The polymeric nanofibers can be loaded with different drugs to be used in the drug delivery systems (DDSs) which supposed to be transdermal, fast dissolving and implantable [37-39]. Two main factors which define drug release specifications are interactions between polymer and loaded drug as well as the diameter of nanofibers. These so called two dimension nanofibers with macroscopic length and microscopic diameters [40] makes this medicated ultrafine fibers useful in both the nanoscale DDS in the transformation of the biopharmaceutics and pharmacokinetics specification of the drug molecules for desirable clinical results. It also makes the processing, packaging, and shipment of the drugs very facile for the common solid dosage [41, 42].

Many antibiotics have the capability to be utilized in FDDSs [43]. Many of these antibiotics such as amoxicillin trihydrate [44], cefuroxime axetil [45] and azithromycin dehydrate [46] are used in fast dissolving tablets. Among these antibiotics, trimethoprim (TMP) as an antibacterial agent is utilized in combination with sulphamethoxazole for the treatment of various infections, reported as a prototype for the provision of antibiotic-containing bandages and their use for treating wounds.

Here TMP, 5-(3,4,5-Trimethoxybenzyl) pyrimidine-2,4-diamine, (Fig. 3) has been used to load into the nanofibers. TMP is widely used in the prophylaxis and treatment of urinary and intestinal infections, senile chronic bronchitis, bacillary dysentery, enteritis, typhus, malaria and respiratory infections. It is often combined with sulfonamides (such as sulfamethoxazole) in pharmaceutical preparations to achieve synergetic effects [47].

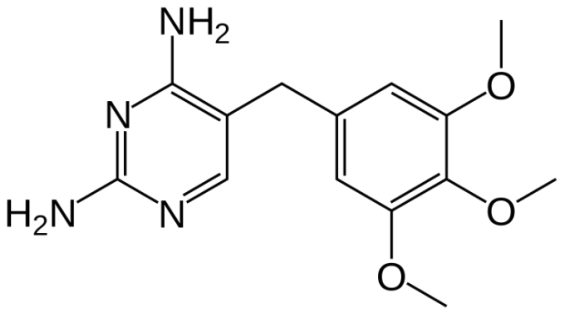

Fig 3. Chemical structure of trimethoprim.

Gupta et al. [48] introduced the solid dispersion (SD) method to increase dissolution and absorption of TMP. They had co-precipitated TMP using polyethylene glycols and PVP as carriers and chloroform as solvent and investigated the solubility enhancement of TMP. Apart from advantages, SD has two major drawbacks. First, the solvent is completely removed from viscose co-precipitations during drying and, secondly, SD process normally has incomplete outputs due to the fact that it mainly relies on pharmaceutical excipients, thus, they should be converted into concrete dosage forms when injected in patient's

body [49]. Using nanostructured materials could help to overcome the problems of the SD method.

In this study, ES technique has been used to fabricate mats of PVP nanofibers as an antibiotic delivery system loaded with TMP. The preparation of these mats will help to improve the water solubility of this drug, and could be particularly beneficial for the treatment of children with urinary infections.

Based on our knowledge, there are very limited publication and reports in literature explaining electrospun antibiotic-loaded nanofibers aimed for FDDSs. Therefore, we have tried to characterize different properties of this system. Scanning electron microscopy (SEM) has been used for morphology characterization and measurement of diameters on nanofibers as a key parameter of fabricated mats. Fourier-transform infrared (FTIR) technique is utilized to study the crystallographic and compositional characterization and differential thermal analysis (DTA) for examination of the thermal behavior of PVP nanofibers. The optical absorbance of samples was measured using UV-Vis spectrophotometer (Cary50, Varian, USA) to calculate the concentration of the samples. Also, *In-vitro* bacterial inhibition test was carried out to determine the activity of the released antibiotic in comparison with conventional solution-cast PVP films.

The main objective of this study is to explore the targeting delivery of the mats of electrospun TMP-loaded PVP nanofibers as an antibiotic delivery system toward the infected cells as well as enhancing their physicochemical traits. Dissolution and absorption of TMP and the transformation capability of TMP-loaded nanofibers as peroral slim films have also been investigated.

MATERIALS AND METHODS

Reagents

TMP (water solubility 0.4 mg/mL) was provided by Behdashtkar Co. (Rasht, Iran). PVP K90 with an average molecular weight of ~1000 kDa was provided by Rahavard Tamin Co. (Tehran, Iran). *Escherichia coli* (ATCC: 35218) and *Staphylococcus aureus* (ATCC: 33591) were purchased from Pasteur Institute (Tehran, Iran). Ethanol 96 %, sodium acetate 3 hydrate, glacial acetic acid, Mueller-Hinton agar (product no. 1054370500), nutrient broth (Cat. No: 6194390500) were purchased from Merck (Darmstadt, Germany). It is worth mentioning that all chemicals were analytically or biologically graded and used without further purification. Also, double distilled water was used for the preparation of all solutions.

Preparation of ES Solutions

Polymeric spinning solutions were prepared by dissolving PVP in ethanol/glacial acetic acid (6:1, v/v) mixed solution. After the dissolution of the polymer, TMP was added into the solution at room temperature (25 °C). The TMP content in spinning solutions was set to be 10 and 20 percent of PVP total weight ($W_{PMP}/W_{PVP} = 10,\ 20\ \%$). This solution was added into a 20 mL plastic syringe (0.5 mm diameter). For ES process, high voltage power supply (30 kV/5mA, Fanavaran nanoazma Ltd., Iran) was applied at 15 kV to the metallic needle. The positive electrode was connected to the metal needle tip and a grounded aluminum foil used as the collector at a distance of 12 cm [12]. Electrospinning was carried out at ambient room temperature in the air condition. The polymer solutions were dispersed through the inner nozzle at the rate of 0.4 mL/h using a double syringe pump SP1000 (Fanavaran nanomeghyas, Iran). The collected nanowebs were dried at 50 °C under vacuum oven for 10 h to eliminate the residual solvents.

Film casting

TMP enclosing PVP films were also fabricated by the casting method to compare the dissolution rate of electrospun nanofibers and films. The spinning solution was cast into a Petri dish with a diameter of 8 cm. After evaporation of the solvents at room temperature and for 48 hours, the films were peeled and stored in clean condition. Additionally, the widths of the films were about 12 mm measured by Pro-Max electronic digital caliper (Mitutoyo, USA). A piece of film equivalent to about 25 mg TMP was used for dissolution tests.

The surface morphologies of drug loaded polymeric nanofibers were studied using a Digital Scanning Electron Microscope (SEM) (KyKy, China). Differential Thermal Analysis (DTA) was carried out using a PYRIS Diamond TG/DTA (PerkinElmer, USA). Sealed samples were heated at 10 °C/min from 20 to 400°C. The nitrogen gas flow rate was 35 mL/min. FTIR spectra were recorded on a Fourier transform IR spectrometer with a KBr pellet (spectrum 1, PerkinElmer, USA). The samples were prepared using the KBr disk method and the scanning range was 400–2000 cm^{-1} with a resolution of 2 cm^{-1}.

Wetting time and dissolution processes

For determination of the wetting time, a layer of filter paper was positioned on a Petri dish with a

diameter of 8 cm. When the paper was completely saturated by distilled water, the excess water was entirely drained out and a section of electrospun nanofibers was carefully placed on the filter paper by a forceps and allowed to wet completely. The time required for complete wetting of the nanofibers was denoted as the wetting time. In addition, a beaker of water was used to evaluate the rate of dissolution of the nanofibrous membranes. The wetting and dissolution processes were recorded at 20 frames per second with a digital video recorder.

In vitro release test

Electrospun nanofibrous membranes were carefully peeled from the aluminum foil and weighed exactly using a digital balance. Electrospun membrane sample and casting film with a weight of 25 mg were separately immersed in 40 mL of artificial saliva [50] at 37 °C, with magnetic stirring at 350 rpm. It must be noted that disintegration of the TMP-loaded membranes in the artificial saliva was very fast (less than 5 sec). 2 mL of prepared samples were collected after 0.5, to 10 minutes with 0.5-minute intervals and after 20 to 120 minutes with 20-minutes intervals and were analyzed by a UV-Vis spectrophotometer. The same amount of fresh water was added to the release system immediately after analyzing by the UV-Vis spectrophotometer, to maintain a constant volume.

Since TMP solution has an absorption peak at 270 nm and PVP has no detectable absorbance at this wavelength, Fig. 4, concentration of TMP/PVP can be calculated by dividing the absorbance of the two solutions at this wavelength. The concentration of TMP in the collected samples could be easily calculated using the calibration curve of pure TMP in acetate buffer pH=5 solution, see Fig. 5.

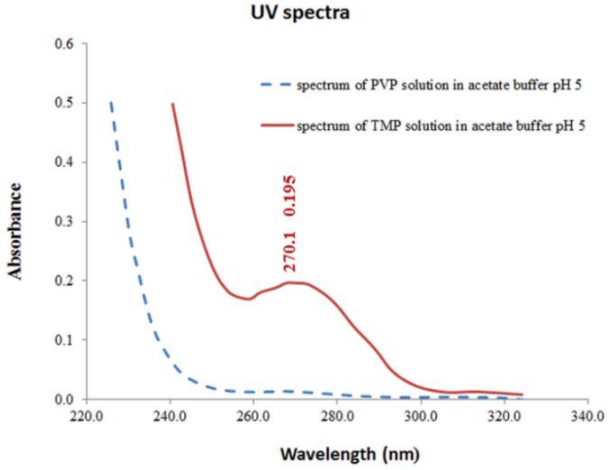

Fig 4. UV- spectra of (a) TMP solution in acetate buffer pH 5, (b) PVP solution in buffer pH 5.

The total assay of the drug in every sample of the electrospun mats or casting film was determined by UV-Vis spectrophotometer after being immersed in artificial saliva for at least 1 hour. Trimethoprim dissolved at specified time periods were plotted as the percentage released versus the time.

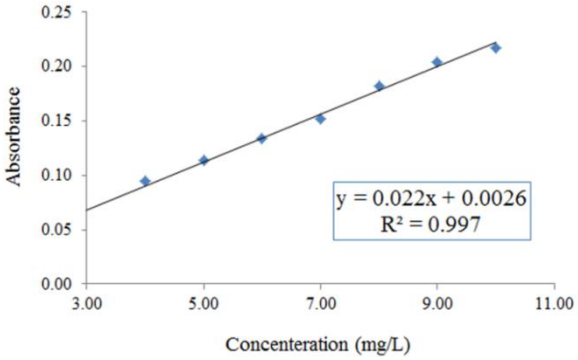

Fig 5. Calibration curve of trimethoprim at maximum 270.1 nm in acetate buffer pH 5.

Microbiological tests

TMP applies antimicrobial activity by inhibiting the reduction of dihydrofolate to tetrahydrofolate, the active form of folic acid, by sensitive organisms. It has a broad antibiotic spectrum that includes gram-negative and gram-positive bacteria [51]. In this study, the antibacterial activity of TMP-loaded PVP nanofibers was investigated using *S. aureus* as a Gram-positive model bacterium and *Escherichia coli* as a gram-negative model bacterium.

Using an antibiotic disk diffusion method, the antimicrobial property of the released PVP nanofibers loaded with TMP on *Escherichia coli* (ATCC: 35218) and *S. aureus* (ATCC: 33591) was determined. To measure the zones of inhibition, *in vitro* studies were performed using the Mueller-Hinton agar (Quelab; Canada). In both cases, first 50 µl of bacterial suspension was transferred to 2 mL of nutrient broth culture medium (beef extract, peptone, Merck Millipore). After 4 hours of initial incubation time, the surface of the solid medium was inoculated with a suspension of these bacterial cultures. McFarland turbidity standard No. 0.5 was used as the bacterial turbidity for the inoculum. In this test, samples (PVP, TMP/PVP (10 %) and TMP/PVP (20 %)) were punched to form circular discs with a diameter of 5 mm. PVP, TMP/PVP (10 %) and TMP/PVP (20 %) samples contained approximately 0, 25, and 50 µg of TMP, respectively. In separate plates samples of PVP, TMP/PVP (10 %) and PVP, TMP/PVP (20 %) were placed on agar plates and incubated at 37 °C for 12 h and 24 h, respectively, allowing the incorporated drugs to diffuse or release from the drug-loaded

mats into the agar. The bacterial inhibition zones of TMP-loaded PVP nanofibrous mats were directly visualized and measured. All tests were performed in triplicate.

In addition, minimum inhibition concentration (MIC) assays were carried out on the above mentioned bacteria. In this test, nutrient broth medium was used as the growth medium. Bacterial suspension was standardized to an absorbance value of 0.2 at 600 nm (8.0×10^7 cells/mL) with a volume of 5 mL. To each aliquot of bacterial suspension, free TMP, drug-loaded nanofiberous mat (TMP/PVP), and non-drug containing sample (PVP nanofibers) were added and, incubated at 37 °C. To evaluate the influence of TMP concentration on the antimicrobial activity, different TMP concentrations (0, 0.1, 0.2, 0.3 and 0.4 μg/mL, respectively) were added into each tube. After incubation, all tested solutions were monitored using a UV-Vis single beam spectrophotometer (Camspec 501, UK) at 600 nm. The absorbance value of the bacterial suspension was correlated directly with the concentration of bacteria in the medium. The bacterial inhibition percentage was calculated according to the following equation:

$$\text{Bacterial inhibition (\%)} = \frac{I_c - I_s}{I_c} \times 100$$

Where I_c and I_s are the absorbance of the control bacterial suspension and the bacterial suspension treated with different samples at 600 nm. Mean and standard deviation of triplicate samples for each sample were reported and all data was expressed as mean ± S.D.

RESULTS

SEM Study

The Surface morphologies of PVP/TMP nanofibers are illustrated in Fig. 6. The SEM images indicate that the concentration of spinning solution and its parameters (distance, electrospinning speed and environment) used were acceptable as the nanofibers produced were cylindrical in shape and smooth, without forming films or beads. The mean fiber diameter is shown in table 1. In comparison, SEM image of casting film of PVP/TMP indicated that the nanofibrous structure of electrospun nanofibers created a high surface to volume ratio and the potential for increasing drug load. The results of fiber diameter analyzes indicate that the increasing concentration of TMP in spinning solutions led to an average rise in fiber diameter that can increase the viscosity of spinning solution of PVP/TMP to 20 % wt.

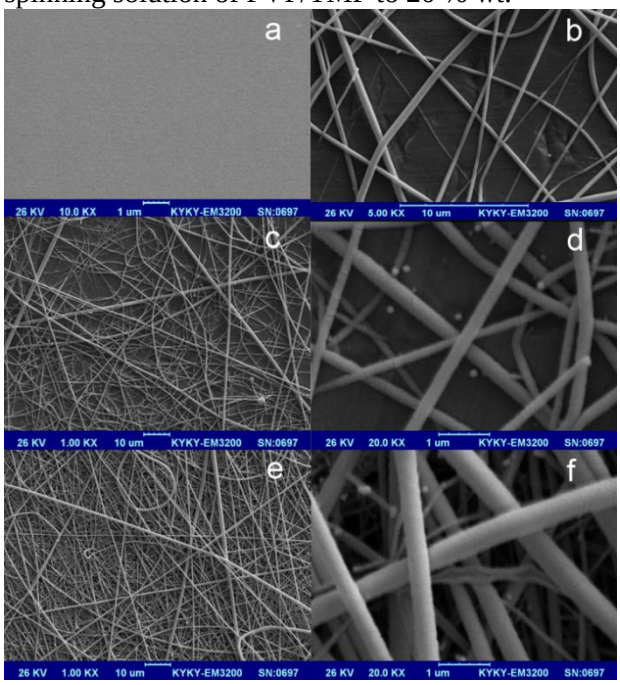

Fig 6. SEM images of (a) PVP/TMP cast film (b) electrospun pure PVP nanofibers (c) electrospun PVP/TMP 10% wt. large scale (d) electrospun PVP/TMP 10% wt. small scale nanofibers (e) electrospun PVP/TMP 20% wt. large scale (f) electrospun PVP/TMP 20% wt. small scale.

Physical status and compatibility of components

The DTA curve of pure TMP exhibited a single endothermic response corresponding to its melting point of 203°C (ΔH_f= − 523.34 ±1.19 kJ mol^{-1}). Being an amorphous polymer, PVP and TMP did not show any phase transitions or fusion peaks. DTA thermograms of the PVP nanofibers loaded by TMP did not show any peaks characteristic of TMP, suggesting that the drug was no longer present as a crystalline material; however, it had been converted into an amorphous state in all the nanofibers (Fig. 7).

Table 1. Fiber diameters.

Nanofibers composition	Fiber diameter (nm)
electrospun pure PVP nanofibers	238.7 ± 83
electrospun TMP/PVP 10 % wt.	219.3 ± 39
electrospun TMP/PVP 20 % wt.	347.9 ± 109

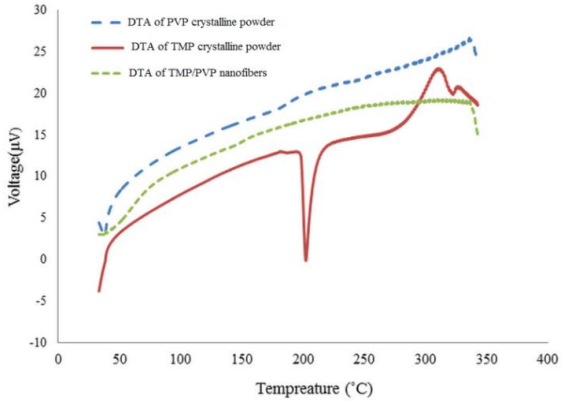

Fig 7. Differential Thermal Analysis thermogram of (a) PVP, (b) pure TMP (c) PVP/TMP electrospun nanofibers.

FT-IR spectroscopy

The infrared spectra (Fig. 8) show the characteristic peaks of trimethoprim at 1623 cm^{-1} (N-H stretching), 1560 cm^{-1} (aromatic C=C stretching), 1425 cm^{-1} (Amine C-N stretching), 1124 cm^{-1}(etheric C-O stretching), and 1494 cm^{-1} (Alkane C-H bending). The PVP spectrum shows the bands at 1661 cm^{-1} (C=O stretching), 1423 cm^{-1} (C-N stretching), 1288 cm^{-1} (-CH bending), 933 cm^{-1} (C-C breathing) and 650 and 576 cm^{-1} (N-C=O bending). The electrospun nanofibers showed no difference in the characteristic FTIR molecular mode in comparison with the individual compounds. The above data suggest that there are no physical or chemical interactions between PVP and TMP in the electrospun nanofibers.

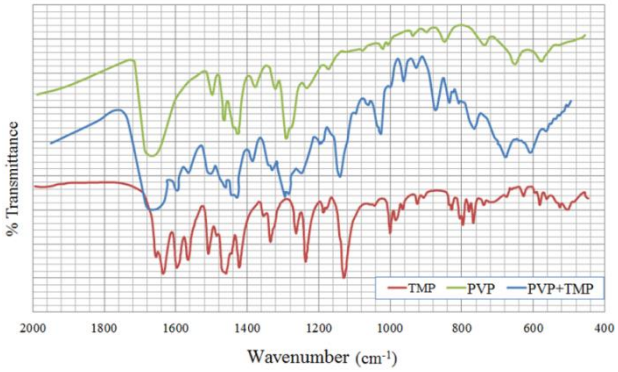

Fig 8. FTIR Spectra of PVP, PVP/TMP nanofibers and TMP.

Pharmacotechnical properties wetting and disintegrating times

The disappearance time of the samples in water was less than 5 s for electrospun PVP/ TMP (10 %) wt. and electrospun PVP/TMP (20 %) wt. Time of disappearance increased slightly as the function of increasing drug content but all electrospun samples fulfilled the requirement of fast dissolution (<30 s) (Fig. 9a).

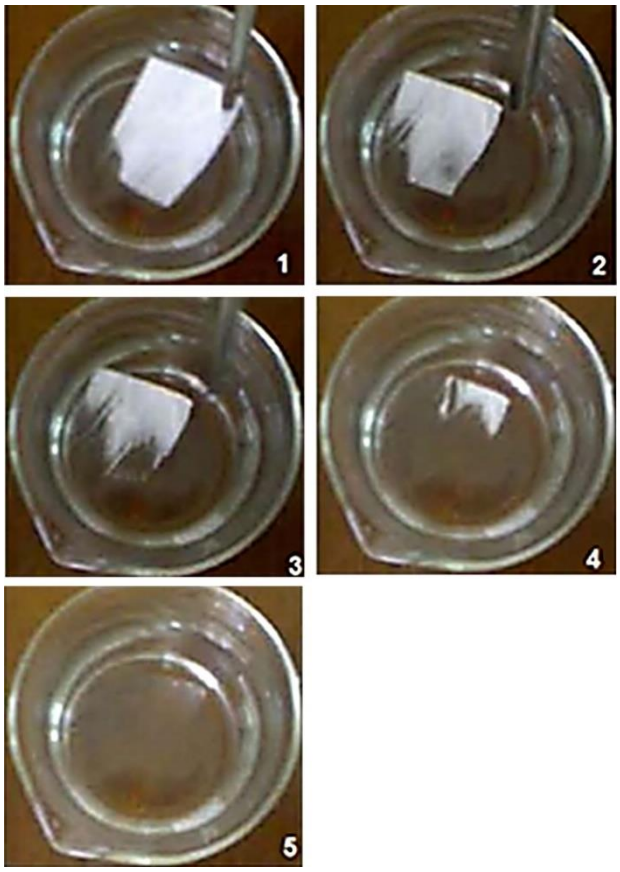

Fig 9.(a) Photographs of the disintegration process of the TMP-loaded PVP fibers, shown in sequence from 1 to 6 (with times keeps of 2 s).

As shown in Fig. 9b, the TMP polymeric nanofibrous mats quickly formed a transparent, 'gel-like' structure and lost their original white color after absorbing water from the wet paper. The wetting time was 6 s and 4 s for electrospun TMP / PVP (20 %) and electrospun TMP / PVP (10 %) wt., respectively. Also, the wet filter paper used in this research aimed to mimic the moisture available in the mouth. Thus, electrospun nanofibers possess an extremely highly porous structure, which can allow rapid penetration of saliva into the pores when placed in the oral cavity. This property can be attributed to high PVP solubility, the high degree of dispersal of TMP in the fiber and the high surface area of the fibers. These results show that electrospun PVP fibers have the potential for creating fast-dissolving DDSs for even exceptionally poorly water-soluble drugs and their derivatives.

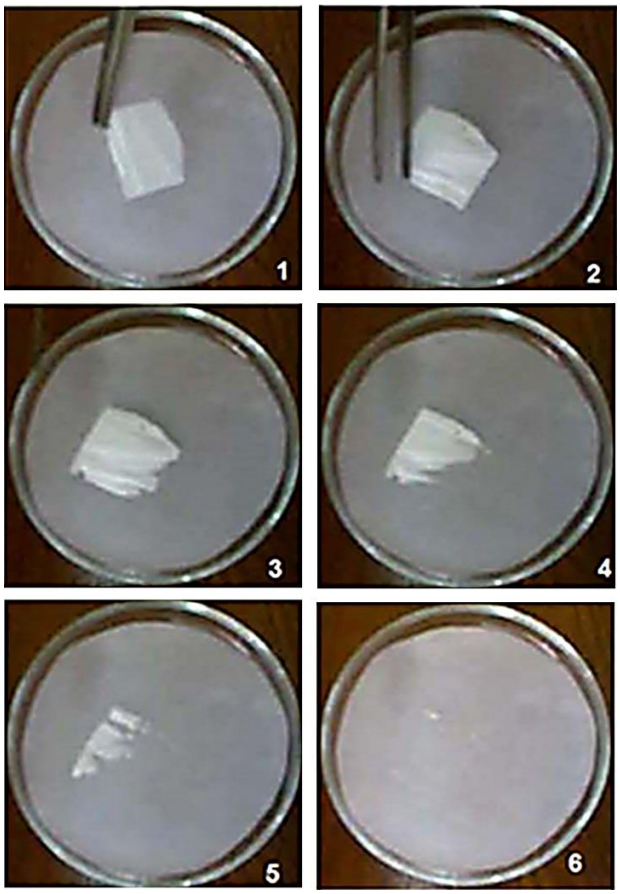

Fig 9.(b) Photographs of the wetting process of the TMP-loaded PVP fibers, shown in sequence from 1 to 6 (with times keeps of 6s).

In vitro dissolution tests

The prepared drug-loaded samples of described morphology were considered promising for oral dissolution because of good water solubility of the applied fiber-forming polymer and the huge surface of the formed fibers**.**

Figures 10 and 11 show the drug release profiles of electrospun webs of cast films with the same composition of electrospun TMP/PVP membranes. For TMP/PVP (10 %) and (20 %) more than 85 % and 84 % of the TMP was released within the first 30 s, respectively. After 60 s, more than 90 % of the TMP contained in these electrospun membranes were released into the dissolution medium, while only 53 % and 65 % of the TMP were released from PVP casting films during the same time respectively. The noteworthy difference between the rates of dissolution of different samples is well recognizable. The sustained release of TMP from PVP films was obtained for up to 5 min, indicating that the drug was released much more slowly and in a relatively steady manner. Dissolution of cast films was dependent on their drug content. Besides, drug release of TMP/PVP (20 %) cast films was significantly faster than that of TMP/PVP (10 %). It is probable that the TMP present in the membrane as TMP acetate salt acts as a small molecule with good water solubility and can easily solubilize, while PVP dissolves more slowly as a macromolecule due to its long polymer chains which are less plasticized because of the presence inter- and intramolecular H-bonds. This means that PVP has a retardant effect, except in cases when the formation of a huge surface area decreases the value of the bulk entangled structure.

The electrospun webs, independently from their drug concentration, were immediately dissolved after immersion in dissolution media owing to the huge surface area. The fast release or dissolution rate of TMP from the nanofibers is due to the high specific surface area, facilitating fast drug release, and the high porosity of the nanofibers, which are able to facilitate the dissolution of the drug in the medium. Moreover, the excellent wettability of the polymer nanostructure causes a rapid penetration of water into the nanopores, promoting a remarkably fast drug release (within a few seconds).

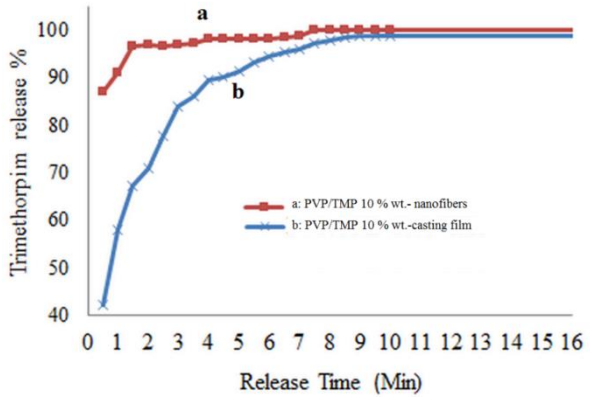

Fig 10. In vitro release profiles of 10 %TMP from (a) PVP nanofibers, (b) PVP casting film. The samples were released in artificial saliva at 37°C.

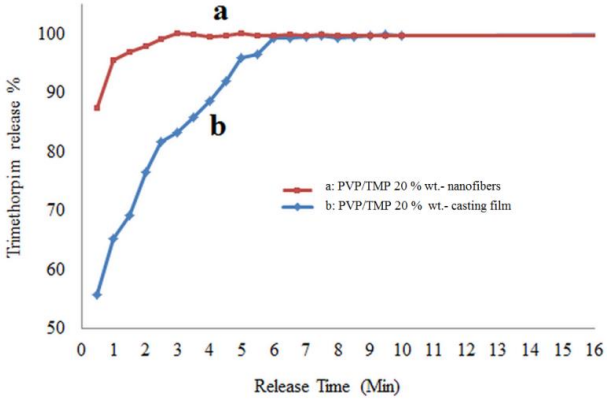

Fig 11. In vitro release profiles of 20 %TMP from (a) PVP nanofibers, (b) PVP casting film. The samples were released in artificial saliva at 37°C.

Microbiological tests

Bacterial inhibition efficacy of the TMP-medicated nanofibrous mats on *S. aureus and*

Escherichia coli was evaluated using an antibiotic disk diffusion method (Fig. 12). After incubation of *S. aureus* and *Escherichia coli* for 12 h and 24 h, respectively, the agar regions with medicated scaffolds displayed uniformly circular visible bacterial inhibition rings. Measured zones of inhibition around the disks for samples are summarized in Tables 2 and 3. These results indicate that the antibiotic drug TMP is released from the medicated nanofibrous mats and diffused onto the agar, thereby, effectively inhibiting bacterial growth. In addition, the antibacterial ability of the TMP-medicated scaffolds could still be observed after 24 h of incubation**.**

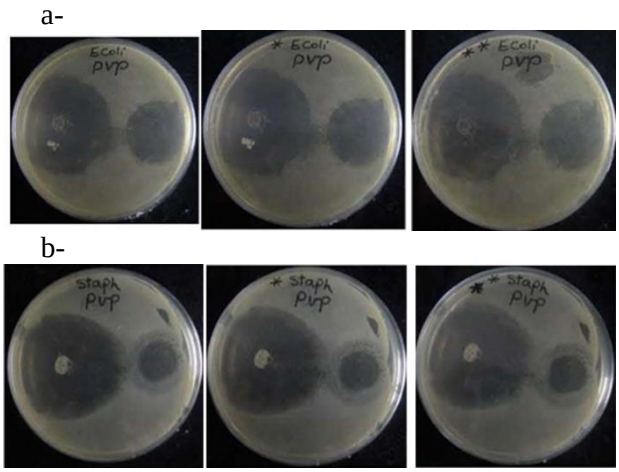

Fig 12. Digital images of the zones of inhibition against (a) *E. coli* observed after 6-h, 12-h (plate is indicated with a star), and 24-h (plate is indicated with 2 stars (b) *S. aureus*, observed after 6-h, 12-h (plate is indicated with a star), and 24-h (plate is indicated with 2 stars). Inhibition zones in the right of each plate is related to control mats in which (no) antibiotic and Inhibition zones in the left of each plate is related to TMP mats antibiotic content 10 wt % of the polymer weight.

Also in this work, the antibacterial activity of TMP-loaded PVP nanofiber was investigated using *Escherichia coli* and *staphylococcus aureus* as model Gram negative and Gram positive bacteria, respectively.

Figure 13 shows the bacterial inhibition percentages after 24 h incubation with different concentrations of free TMP. *Escherichia coli* is more sensitive to TMP and bacterial inhibition occurs at 0.4 µl/mL. Degree of E. *coli* and S. *aureus* inhibition was 83% and 71% respectively.

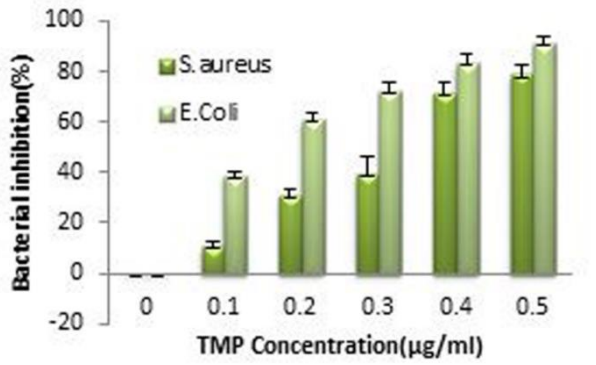

Fig 13. Inhibition of bacterial (*Escherichia coli and S. aureus*) growth after 24 h of incubation.

In both bacterial strains, TMP and TMP/PVP nanofiber exhibit equal bacterial inhibition and little difference between the two strains was evident.

Bacterial inhibition percentages after incubation of the bacterial suspension with different samples were shown in Fig. 14. Clearly, the sample without TMP encapsulation (PVP nanofiber) does not display significant effect on bacterial growth. In contrast, free TMP powder and drug-loaded nanofiber mat (TMP/PVP) were able to inhibit bacterial growth.

The results show that the medicated TMP/PVP composite nanofibers could be effective in inhibiting the growth of bacteria and have the potential to be used in wound dressing and tissue engineering.

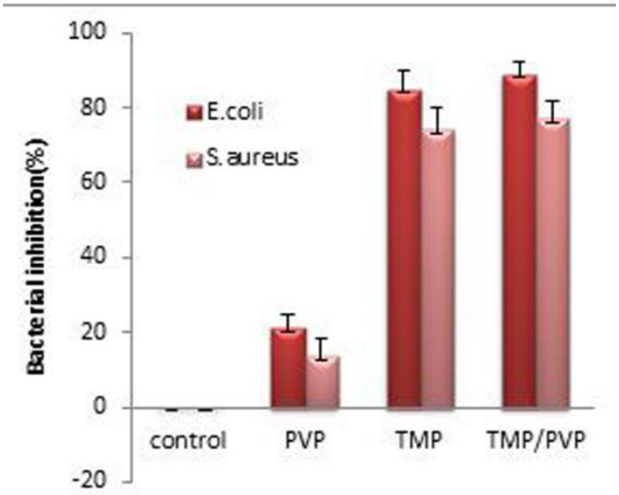

Fig 14. Inhibition of bacterial (*Escherichia coli* and *S. aureus*) growth after 24 h of incubation with free TMP, TMP/PVPs and PVP nanofiber. The concentration of free TMP and TMP in medicated sample was 0.4 µg/mL.

Table 2. Determination of bacterial inhibition efficacy of the TMP-medicated nanofibrous mats (TMP 10%) on *Escherichia coli.*

Incubation time	Inhibition zone for control mat (PVP) (mm)	Inhibition zone for sample mat (TMP/PVP) (mm)	Effective inhibition zone for sample mat (TMP/PVP) (mm)
6 h	25	39	14
12 h	27	43	16
24 h	24	38	14

Table 3. Determination of bacterial inhibition efficacy of the TMP-medicated nanofibrous mats (TMP 10%) on *S. aureus*.

Incubation time	Inhibition zone for control mat (PVP) (mm)	Inhibition zone for sample mat (PVP/TMP) (mm)	Effective inhibition zone for sample mat (PVP/TMP) (mm)
6 h	17	41	24
12 h	16	40	24
24 h	14	39	25

CONCLUSIONS

This work dealt with fast-dissolving drug delivery systems derived from electrospun PVP nanofibers and trimethoprim as a model drug. It has been shown the possibility of one-step preparation of fibrous materials from PVP loaded with trimethoprim using electrospinning.

Ultrafine nanofibers with average diameters of 220 to 350 nm and smooth surfaces were synthesis using electrospinning technique.

10 % and 20 % wt TMP/PVP drug delivery system with molecular level integration and good compatibility with no interaction between polymer and drug, has been prepared which confirmed by DTA, FTIR and SEM analysis. Pharmacotechnical tests showed that TMP/PVP nanofibrous mats had almost the equal dissolution time, about 2 s, and wetting time, about 5 s. The release measurements from the PVP nanofibrous matrices showed that the drugs can rapidly dissolve in water in a burst manner. Bioactivity studies showing that the antibacterial properties of TMP are preserved in nanofiber form.

The obtained results showed that PVP/antibiotic mats are suitable for applications that require an initial burst release of the active substances, for instance in wound dressing devices, for inhibition of pathogenic microorganisms invasion and bacterial biofilm formation.

These results proving that TMP-loaded PVP electrospun nanofibers are potentially the great candidate for implication in fast-dissolving drug delivery systems, although more research and studies are essential for the decisive approval.

Acknowledgments: *The authors would like to express their thanks to the Behdashtkar Drug Company for financial support.*

REFERENCES

1. D. G. Yu, L. M. Zhu, K. White , C. Branford,, *Health*, **1,** 67 (2009).
2. X. Hu, S. Liu, G. Zhou, Y. Huang, Z. Xie, X. Jing, *Journal of Controlled Release*, **185**, 12 (2014) .
3. T. Potrč, S. Baumgartner, R. Roškar, O. Planinšek, Z. Lavrič, J. Kristl, P. Kocbek, *Eur. J. Pharmac. Sci*., **75**, 101 (2015).
4. A. C. Liang, L. I. H. Chen, *Expert Opinion on Therapeutic Patents*, **11**, 981 (2001).
5. V. Pillay, C. Dott, Y. U. Choonara, C. Tyagi, L. Tomar, P. Kumar, L. C. Du Toit, V. M. K. Ndesendo, *Journal of Nanomaterials*, **2013**, Article ID 789289 (2013).
6. D. G. Yu, X. Wang, X. Y. Li, W. Chian, Y. Li, Y. Z. Liao, *Acta Biomaterialia*, **9**, 5665 (2013).
7. A. Farooq, M. Yar, A. S. Khan, L. Shahzadi, S. A. Siddiqi, N. Mahmood, A. Rauf, Z. A. Qureshi, F. Manzoor, A. Chaudhry, I. Rehman, *Materials Science and Engineering: C*, **56**, 104 (2015).
8. G. Gainza, S. Villullas, J. L. Pedraz, R. M. Hernandez, M. Igartua, *Nanomedicine: Nanotechnology, Biology and Medicine*, **11**, 1551 (2015).
9. S. Um-i-Zahra, X. Shen, H. Li, L. Zhu, *Journal of Polymer Research*, **21**, 1 (2014).
10. K. H. Zhang, Q. Z. Yu, X. M. Mo, *International Journal of Molecular Sciences*, **12**, 2187 (2011).
11. S. Kunte, P. Tandale, *J Pharm Bioallied Sci.*, **2**, 325 (2010).
12. U. E. Illangakoon, H. Gill, G. C. Shearman, M. Parhizkar, S. Mahalingam, N. P. Chatterton, G. R. Williams, *International Journal of Pharmaceutics*, **477**, 369 (2014).
13. H. Yang, S. Kim, I. Huh, S. Kim, S. F. Lahiji, M. Kim, H. Jung, *Biomaterials*, **64**, 70 (2015).
14. D. Li, Y. Xia, *Advanced Materials*, **16**, 1151 (2004)
15. J. Doshi, D. H. Reneker, *Journal of Electrostatics*, **35**, 151 (1995)
16. J. M. Deitzel, J. Kleinmeyer, D. Harris, N. C. Beck Tan, *Polymer*, **42**, 261 (2001).

17. E. R. Kenawy, G. L. Bowlin, K. Mansfield, J. Layman, D. G. Simpson, E. H. Sanders, G. E. Wnek, *Journal of Controlled Release*, **81**, 57 (2002).
18. M. Sadri, S. Arab-Sorkhi, H. Vatani, A. Bagheri-Pebdeni, *Fibers and Polymers*, **16**, 1742 (2015).
19. A. Zarghami, M. Irani, A. Mostafazadeh, M. Golpour, A. Heidarinasab, I. Haririan, *Fibers and Polymers*, **16**, 1201 (2015).
20. T. He, J. Wang, P. Huang, B. Zeng, H. Li, Q. Cao, S. Zhang, Z. Luo, D. Y. B. Deng, H. Zhang, W. Zhou, *Colloids and Surfaces B: Biointerfaces*, **130**, 278 (2015).
21. X. Li, M. A. Kanjwal, L. Lin, I. S. Chronakis, *Colloids and Surfaces B: Biointerfaces*, **103**, 182 (2013).
22. F. Ignatious, L. H. Sun, C. P. Lee, J. Baldoni, *Pharmaceutical Research*, **27**, 576 (2010).
23. M. Jelvehgari, P. Zakeri-Milani, M. R. Siahi-Shadbad, B. D. Loveymi, A. Nokhodchi, Z. Azari, H. Valizadeh, *AAPS PharmSciTech*, **11**, 1237 (2010).
24. Y. J. Yamanaka, K. W. Leong, *Journal of Biomaterials Science Polymer Edition*, **19**, 1549 (2008).
25. A. Balogh, R. Cselkó, B. Démuth, G. Verreck, J. Mensch, G. Marosi, Z. K. Nagy, *International Journal of Pharmaceutics*, **495**, 75 (2015).
26. B. Sun, Y. Z. Long, H. D. Zhang, M. M. Li, J. L. Duvail, X. Y. Jiang, H. L. Yin, *Progress in Polymer Science*, **39**, 862 (2014).
27. J. Choi, H. Kim, H. Yoo, *Drug Delivery and Translational Research*, **5**, 137 (2015).
28. B. P. Antunes, A. F. Moreira, V. M. Gaspar, I. J. Correia, *Carbohydrate Polymers*, **130**, 104 (2015).
29. M. F. Oliveira, D. Suarez, J. C. B. Rocha, A. V. N. de Carvalho Teixeira, M. E. Cortés, F. B. De Sousa, R. D. Sinisterra, *Materials Science and Engineering: C*, **54**, 252 (2015).
30. X. Wu, C, Branford-White, L, Zhu, N. P. Chatterton, D. Yu, J*ournal of Materials Science: Materials in Medicine*, **21**, 2403 (2010).
31. A. Toncheva, D. Paneva, V. Maximova, N. Manolova, I. Rashkov, *European Journal of Pharmaceutical Sciences*, **47**, 642 (2012).
32. Z. K. Nagy, A. Balogh, B. Vajna, A. Farkas, G. Patyi, A. Kramarics, G. Marosi, *Journal of Pharmaceutical Sciences*, **101**, 322 (2012).
33. A. Rogina, *Applied Surface Science*, **296**, 221 (2014).
34. H. Brooks, N. Tucker, *Polymer*, **58**, 22 (2015).
35. L. Palangetic, N. Reddy, S. Srinivasan, R. E. Cohen, G. H. McKinley, C. Clasen, *Polymer*, **55**, 4920 (2014).
36. L. Dan, X. Younan, *Nano Letters*, **4**, 933 (2004).
37. Z. M. Huang, Y. Z. Zhang, M. Kotaki, S. Ramakrishna, *Composites Science and Technology*, **63**, 2223 (2003).
38. X. X. Shen, D. G. Yu, C. B. Ranford-White, L. M. Zhu, Preparation and characterization of ultrafine eudragit L100 fibers via electrospinning, in: The 3rd International Conference on Bioinformatics and Biomedical Engineering Shanghai, China, 2008.
39. X. Xu, X. Chen, Z. Wang, X. Jing, *European Journal of Pharmaceutics and Biopharmaceutics*, **72**, 18 (2009).
40. D. G. Yu, X. F. Zhang, X. X. Shen, C. Brandford-White, L. M. Zhu, *Polymer International Journal of ChemTech Research*, **58**, 1010 (2009).
41. Y. Dzenis, *Science*, **304**, 1917 (2004).
42. X. Chen, H. Yan, W. Sun, Y. Feng, J. Li, Q. Lin, Z. Shi, X. Wang, *Polymer Bulletin*, **72**, 3097 (2015).
43. K. Kavitha, K. Subramaniam, B. J. Hui, K. Santhi, S. Dhanaraj, M. Rupesh Kumar, *Research Journal of Pharmaceutical, Biological and Chemical Sciences*, **4**, 1510 (2013).
44. S. Kamal, K. Gautam, P. Yash, International Journal of pharma and bio sciences, **4**, 254 (2013).
45. N. Bhandari, N. B. Gupta, *Journal of Drug Discovery and Therapeutics*, **1**, 27 (2013).
46. S. W. Ravi, S. M. Ravikant, *Pharmacie Globale*, **4**, 1 (2012).
47. R.B. Patel, P. G. Welling, *Clinical Pharmacokinetics*, **5**, 405 (1980).
48. R. L. Guptat, R. Kumar, A. K. Singla, *Drug Development and Industrial Pharmacy*, **17**, 463 (1991).
49. D. Paramita, M. Sabyasachi, *Biology and Medicine*, **1**, 2 (2010).
50. K. Arvidson, E. G. Johansson, *European Journal of Oral Sciences*, **93**, 467. (1985)
51. R. Gleckman, N. Blagg, D. W. Joubert, *The Journal of Human Pharmacology and Drug Therapy*, **1**, 14 (1981).